NIH Public Access
Author Manuscript
Med Mycol. Author manuscript; available in PMC 2013 March 25.

Published in final edited form as:
Med Mycol. 2013 January ; 51(1): 93–102. doi:10.3109/13693786.2012.699685.

Blastomyces dermatitidis septins *CDC3, CDC10*, and *CDC12* impact the morphology of yeast and hyphae, but are not required for the phase transition

AMBER J. MARTY[*] and **GREGORY M. GAUTHIER**[†]

[*]Department of Medicine, University of Wisconsin, Madison, Wisconsin, USA

[†]Division of Infectious Diseases, Department of Medicine, University of Wisconsin, Madison, Wisconsin, USA

Abstract

Blastomyces dermatitidis , the etiologic agent of blastomycosis, belongs to a group of thermally dimorphic fungi that change between mold (22°C) and yeast (37°C) in response to temperature. The contribution of structural proteins such as septins to this phase transition in these fungi remains poorly understood. Septins are GTPases that serve as a scaffold for proteins involved with cytokinesis, cell polarity, and cell morphology. In this study, we use a GFP sentinel RNA interference system to investigate the impact of *CDC3, CDC10*, *CDC12*, and *ASPE* on the morphology and phase transition of *B. dermatitidis*. Targeting *CDC3*, *CDC10*, and *CDC12* by RNA interference resulted in yeast with aberrant morphology at 37°C with defects in cytokinesis. Downshifting the temperature to 22°C promoted the conversion to the mold phase, but did not abrogate the morphologic defects. *CDC3, CDC10*, and *CDC12* knockdown strains grew as mold with curved, thickened hyphae. Knocking down *ASPE* transcript did not alter morphology of yeast at 37°C or mold at 22°C. Following an increase in temperature from 22°C to 37°C, all septin knockdown strains were able to revert to yeast. In conclusion, *CDC3, CDC10*, and *CDC12* septin-encoding genes are required for proper morphology of yeast and hyphae, but are dispensable for the phase transition.

Keywords

dimorphic fungi; septin; phase transition; morphogenesis

Introduction

Blastomyces dermatitidis, the etiologic agent of blastomycosis, belongs to a group of human pathogenic fungi that exhibit thermal dimorphism [1]. These organisms, which include *Histoplasma capsulatum*, *Coccidioides* spp., *Paracoccidioides brasiliensis*, *Sporothrix schneckii*, and *Pencillium marneffei*, undergo a reversible, temperature-dependent shift in their morphology known as phase transition [1]. In the environment (22°C), they grow as molds and produce infectious conidia. Following the disruption of soil, aerosolized mycelial

© 2012 ISHAM

Correspondence: Gregory M. Gauthier, MD, MS, Assistant Professor (CHS), Department of Medicine, Division of Infectious Diseases, University of Wisconsin, Madison, 1550 Linden Drive, Microbial Sciences Building, Room 4301, Madison, WI 53706, USA. Tel: 31 608 262 7703; fax: 3 1 608 263 4464; gmg@medicine.wisc.edu.

Declaration of interest: The authors report no conflicts of interest. The authors alone are responsible for the content and writing of the paper.

NIH-PA Author Manuscript
NIH-PA Author Manuscript
NIH-PA Author Manuscript

NIH-PA Author Manuscript

NIH-PA Author Manuscript

NIH-PA Author Manuscript

fragments and conidia that are inhaled into the lungs of a mammalian host (37°C) convert into pathogenic yeasts (or spherules for *Coccidioides* spp.) to cause disease [1–3]. Collectively, the dimorphic fungi infect several million people each year, including persons with either intact or impaired immune defenses [4,5]. Clinical manifestations are heterogeneous and include subclinical illness, pneumonia, acute respiratory distress syndrome, and disseminated disease [1,5].

The conversion between mold and yeast is a complex process that requires the fungal cell to sense changes in temperature and undergo a radical rearrangement in morphology [1]. Our understanding of how the phase transition is regulated is limited to only a handful of genes including those that alter intracellular signaling or transcription including *DRK1*, *RYP1-3*, and *SREB* [6–10]. The impact of genes that encode ultrastructural proteins such as septins, remains largely unexplored in the endemic dimorphic fungi. Septins are GTP-binding proteins that form heteroligomeric complexes at sites of bud formation in yeast and growth at the hyphal tips in filamentous fungi [11–13]. Septin complexes serve as a scaffold to facilitate localization of proteins involved with cytokinesis and cell polarity [11]. In fungi such as *Saccharomyces cerevisiae*, septins also form a barrier to prevent back-diffusion of proteins from the daughter to the mother cell [11]. In several fungi including *S. cerevisiae*, *Ustilago maydis*, *Cryptococcus neoformans*, and *Candida albicans*, the impact of septins on morphology can be influenced by temperature [14–17]. The link between morphology and temperature involving septins has yet to be fully elucidated in the dimorphic fungi.

In this study, we use RNA interference to investigate the impact of septin-encoding genes *CDC3*, *CDC10*, *CDC12*, and *ASPE* on the morphology and phase transition of *Blastomyces dermatitidis*. This research expands upon our analysis of *B. dermatitidis CDC11* on morphogenesis [12]. We found that *B. dermatitidis* strains knocked down for *CDC3*, *CDC10*, and *CDC12* grow as misshapen yeast at 37°C and aberrant hyphae at 22°C. Knocking down *ASPE* transcript did not impact the morphology of yeast or hyphae. Knockdown strains did not exhibit defects in thermotolerance and were able to convert between mold and yeast.

Materials and methods

Strains and media

Transformants were generated from a reporter strain of *B. dermatitidis* that was engineered to express green fluorescent protein (GFP) [12]. This strain, T53-19 GFP, was derived from ER-3 (ATCC MYA-2586), which forms conidia but is hypovirulent in a murine model of infection [6]. GFP expression in the reporter is driven by the BAD1 promoter, which is expressed at 37°C, but not 22°C [12]. The H2AB promoter, which is active at 37°C and 22°C when analyzed by quantitative real-time PCR (data not shown), drives transcription of the RNA hairpin responsible for RNA interference. The GFP reporter strain and transformants were grown on 3M medium [18] or *Histoplasma* macrophage medium (HMM) [19], with or without supplementation with 100 μg/ml hygromycin B (AG Scientific, San Diego, CA) at 37°C and 22°C. Liquid HMM, with or without supplementation with 100 μg/ml hygromycin B, was used for the growth of yeast and mold phases at 37°C and 22°C, respectively. *Agrobacterium tumefaciens* strain LBA1100 harboring the Ti helper plasmid pAL1100 (gift from C. van den Hondel; Leiden University, The Netherlands) was maintained on Luria-Bertani (LB) medium supplemented with 0.1% glucose, spectinomycin 100 μg/ml, and kanamycin 100 μg/ml following transformation with a binary vector [20].

NIH-PA Author Manuscript
NIH-PA Author Manuscript
NIH-PA Author Manuscript

Transformation of *B. dermatitidis* GFP reporter strain

Agrobacterium-mediated DNA transfer was used to transform T53-19 GFP reporter strain with vectors targeting *CDC3*, *CDC10*, *CDC12*, and *ASPE* for RNA inferference (RNAi). Control strains were transformed with pH2AB, which only targeted *GFP* (GFPi-only control), or pBTS4, which lacked an RNAi construct (non-RNAi vector control). For each septin gene, two separate, non-overlapping regions in the open reading frame (ORF) were targeted for RNAi (Fig. 1). Primer design was based on the sequenced genome of *B. dermatitidis* strain SLH14081 (www.broadinstitute.org). Primers used to amplify the septin loci targeted for RNAi were as follows:

1. *CDC3* 5′ locus forward (*CDC3* 5′ F) GGGGAC AAGTTTGTACAAAAA-AGCAGGCTtgttcgtcgcaagttgaccg and reverse (*CDC3* 5′ R) GGGGACC ACTTTGTACAAGAAAGCTGGGTTGGGTTGGATAAAGTAGACACAGGC;
2. *CDC3* 3′ locus forward (*CDC3* 3′ F) GGGGAC A AG T T T G TAC A A A A A AG C AG G C T T C GCTAAGGCTGATACTCTCACCG and reverse (*CDC3* 3′ R) GGGGACCACTTTGTACAAGAAAGCTGGGTCGCTCTTCTTCCTGTTTGAC CG;
3. *CDC10* 5′ forward (*CDC10* 5′ F) GGGGACAA GTTTGTACAAAAAAGCAGGCTAGATCGAGCGGAAACTACTGA and reverse (*CDC10* 5′ R) GGGGACCACTTTGTACAAGAAAGCTGGGTG CTGAAAAGGCATTGAGAA;
4. *CDC10* 3′ locus forward (*CDC10* 3′ F) GGGGACA AGTTTGTACAAAAAAGCAGGCTTGATATCGTCGTC-CTGAAGAAAC and reverse (*CDC10* 3′ R) GGGGACCACTTTGTACAAGAAAGCTGGGTGTCGGCTGCCAC-CTGAATGCG;
5. *CDC12* 5′ locus forward (*CDC12* 5′ F) GGGGACA AGTTTGTACAAAAAAGCAGGCTTAGCTCCCAAATCAACGGTATGC and reverse (*CDC12* 5′ R) GGGGACCACTTTGTACAAGAAAGCTGGGTTATCCAGGGGCTTTAGGGT ATGAC;
6. *CDC12* 3′ locus forward (*CDC12* 3′ F) GGGGAC AAGTTTGTACAAAAAAGCAGGCTGTTGCCAAAGCCGATACAC and reverse (*CDC12* 3′ R) GGGGACCACTTTGTACAAGAAAGCTGGGTAAAGTTAGCATTGGCACAT;
7. *ASPE* 5′ locus forward (*ASPE* 5′ F) GGGGACA AGTTTGTACAAAAAAGCAGGCTCTCAAACCGCAAGACGAACA and reverse (*ASPE* 5′ R) GGGGACCACTTTGTACAAGAAAGCTGGGTCACGCAGCTGCAGATCAAC AACAT; and
8. *ASPE* 3′ locus forward (*ASPE* 3′ F) GGGGACA AGTTTGTACAAAAAAGCAGGCTTGCGCGACACTCACATTCACTGC and reverse (*ASPE* 3′ R) GGGGACCACTTTGTACAAGAAAGCTGGGTCTCCATCGCTCGTACCACAC TTTC.

Following PCR amplification using Elongase (Invitrogen, Carlsbad, CA), the amplicons were separated using gel electrophoresis and purified using a QiaQuick PCR purification kit (Qiagen, Valencia, CA). Once sequences of the amplicons were confirmed, RNAi vectors

NIH-PA Author Manuscript

NIH-PA Author Manuscript

NIH-PA Author Manuscript

were constructed using the Gateway cloning system (Invitrogen, Carlsbad, CA) as described by Krajaejun *et al*. [12].

A. tumefaciens transformation of *B. dermatitidis* T53-19 GFP reporter strain was performed as previously described [7]. In brief, 2×10^7 yeast cells were co-cultured with 6×10^8 *A. tumefaciens*, which harbored the RNAi vector, on Biodyne A membranes on induction medium with acetosyringone (IMAS). Following 72 h of incubation at 22°C, the membranes were transferred to 3M medium supplemented with 100 μg/ml hygromycin and 200 μM cefotaxime, and incubated at 37°C. Strains knocked down for *CDC3, CDC10, CDC12,* and *ASPE* were screened for loss of GFP intensity using VersaDoc imaging system (BioRad, Hercules, CA) and fluorescent microscopy (Olympus BX60). Control strains were screened for GFP expression (reporter strain, non-RNAi vector control) or loss of fluorescence (GFPi-only).

Conidial Formation studies

To investigate for defects in spore production, yeast from control and septin RNAi strains were inoculated at a density of 2×10^7 yeast per plate, in duplicate, and incubated at 22°C for 14 days. Conidia were harvested from each plate in phosphate buffered saline by manual disruption [21] and counted using a hemocytometer. Control and knockdown strains formed conidia poorly on 3M medium, which was unexpected because *B. dermatitidis* usually produces abundant conidia on this medium [7]. Subsequent studies used Bird medium to promote conidial production [22].

Quantitative real-time PCR (qRT-PCR)

Total RNA was extracted from control and knockdown strains harvested from 3M agar at 37°C as previously described by Gauthier *et al*. [7]. Following treatment with Turbo DNase (BioRad) and additional purification using an RNeasy kit (Qiagen), total RNA was converted to cDNA using iScript cDNA Synthesis Kit (Bio-Rad). PCR was performed with SsoFast EvaGreen Supermix (Bio-Rad), using a MyiQ real-time PCR detection system (Bio-Rad). Reactions were performed in triplicate. Bio-Rad iCycle conditions were as follows: 1 cycle 95°C × 30 sec, followed by 40 cycles at 95°C for 5 sec, 60°C for 10 sec. Primers used for qRT-PCR were *CDC3* 5′ forward CCCTCTTCAAGCAAAGGATTC and reverse GTTTTCGGCGATGGTTTC; *CDC10* 5′ forward AACGCTCAAATCAAGGACATC and reverse CGCAATG GTTCTCGTCTTC; *CDC11* 5′ forward GGTGGGATG GG GATACAAG and reverse ATCGCTATGTTAGGA AAGGTCTC; *CDC12* 5′ forward ACGCTTCACCGAAC AAGT and reverse TGTTTGATAGCTGCATGAGT; *ASPE* 5′ forward TGGAGGTCTTGACGCTTGAG and reverse CTTGGGCTTGGGCATCAG; alpha-tubulin forward GGTCACTACACCATCGGAAAG and reverse CTGGAG-GGACGAACAGTTG. Transcript abundance of *CDC3, CDC10, CDC12*, and *ASPE* were normalized relative to transcript abundance of alpha-tubulin. Following normalization, data was analyzed using $2^{-\Delta\Delta Ct}$ [23].

Cell staining

B. dermatitidis nuclei were stained using sytox green and visualized using fluorescent microscopy (Olympus BX60). Sytox staining was performed on fixed cells (2% paraformaldehyde for 1 h) as described by Sullivan *et al*. [20]. Cell wall and septal chitin were stained in yeast and mold cells using calcofluor white (Sigma-Aldrich, St. Louis, MO). Cells fixed in 2% paraformaldehyde were washed with phosphate buffered saline (PBS), stained with 0.025 mg/ml of calcofluor white (Sigma-Aldrich, St. Louis, MO) for 30 min at room temperature, and washed three times with PBS containing 0.2% BSA. Stained cells were visualized by fluorescent microscopy using an excitation filter with a range of 400–410 nm.

NIH-PA Author Manuscript

NIH-PA Author Manuscript

NIH-PA Author Manuscript

Statistical analysis

Analysis of variance (ANOVA) was used to compare knockdown septin strains with controls for quantitative abnormalities in morphology and transcript abundance. For analysis of growth rate, repeated measures ANOVA was used. Probability values were adjusted based on the Dunnett's procedure or Tukey's HSD (Honestly Significant Difference).

Results

Identification and characterization of septins in *Blastomyces dermatitidis*

Using tBLASTn to search the sequenced genomes of *B. dermatitidis* strains 26199 (http://genome.wustl.edu/genomes/fungi) and SLH14081 (www.broadinstitute.org), we identified septins from all 5 clades including CDC10 (clade 1A), CDC3 (clade 2A), CDC11 (clade 3), CDC12 (clade 4), and ASPE (clade 5) (Fig. 1) [24]. Similar to other filamentous fungi and pathogenic basidomycetes, the genome of *B. dermatitidis* lacked genes for accessory (*SHS1/SEP7)* and sporulation-regulated (*SPR3*, *SPR8*) septins, as found in *S. cerevisiae*, *Candida* spp., and *Kluyveromyces lactis* [24–28]. We have previously described the percent identity and similarity of the amino acid sequences of *B. dermatitidis* septin homologs to *S. cerevisiae*, *Schizosaccharomyces pombe*, *C. albicans*, and *Aspergillus nidulans* [12]. Subsequent to that publication, the genomes of several dimorphic fungi have been sequenced (www.broadinstitute.org). *B. dermatitidis* septins *CDC3, CDC10, CDC11,* and *CDC12* show a high degree of amino acid identity and similarity with *H. capsulatum*, *P. brasiliensis*, *Coccidioides immitis*, and *Coccidioides posadasii* (Table 1).

Analysis of the predicted amino acid sequences revealed that *B. dermatitidis* septins contained conserved motifs including septin unique elements, sep motifs, polybasic regions, guanine nucleotide binding regions, and coiled-coil domains (Fig. 1). Septin unique elements were identified near the C-terminus for all predicted *B. dermatitidis* septins. The function of this 53 amino acid motif, which is conserved among septin proteins, remains unknown [28]. Similar to septin unique element, *B. dermatitidis* septins possessed Sep1–4 motifs, which are conserved in 86–98% of septins [24]. With the exception of a homolog of ASPE, all *B. dermatitidis* septins had an N-terminal polybasic region, which promotes the binding of septins to plasma membrane phosphoinositides [29]. As expected, *B. dermatitidis* septins contained domains involved with guanidine nucleotide binding, including G1 (GxxxxKG [S/T]), G3 (DxxG), and G4 (NKxD). G1 and G3 domains are predicted to bind the phosphates of GTP, whereas G4 impacts binding specificity [30]. Three *B. dermatitidis* septins, CDC3, CDC11, and CDC12, were predicted to have a C-terminal coiled-coil domain by the multicoil program [31]. The coiled-coil domain facilitates septin-protein interactions and promotes some septin–septin interactions (i.e. Cdc3-Cdc11 in *S. cerevisiae*) [29].

RNAi of *CDC3, CDC10,* and *CDC12* in *B. dermatitidis* results in misshapen yeast at 37°C

To investigate the function of *CDC3*, *CDC10*, *CDC12*, and *ASPE* on *B. dermatitidis* morphology, we knocked down the expression of these genes using a GFP sentinel RNAi system. In this system, RNAi simultaneously reduces transcription of target genes (i.e., *CDC3*) and *GFP*. The loss of GFP fluorescence indicates successful knockdown of the target gene [12]. For each septin gene, two non-overlapping regions were targeted for RNAi (Fig. 1). Strains knocked down for *CDC3*, *CDC10*, and *CDC12* displayed a loss of GFP fluorescence and grew as large, misshapen yeast at 37°C (Fig. 2A). In contrast, *ASPE* knockdown strains and control strains (GFP reporter, non-RNAi vector control, GFPi-only) grew as broad-based budding yeast (Fig. 2A). Quantitative analysis of 3–5 independent knockdowns revealed that the majority of cells (55–85%) for *CDC3*, *CDC10*, and *CDC12*

NIH-PA Author Manuscript

NIH-PA Author Manuscript

NIH-PA Author Manuscript

RNAi strains grew as aberrant yeast (bean-shaped, large ovoid forms, and elongated) when compared to control and *ASPE* RNAi strains (adjusted *p*-value < 0.05; Figs. 2A, 3).

Quantitative real-time PCR (qRT-PCR) demonstrated reduction of transcript abundance for *CDC3*, *CDC10*, *CDC12*, and *ASPE* (Fig. 4). Using the $2^{-\Delta\Delta Ct}$ method, there was a 73% reduction in transcript abundance of *CDC3* for *CDC3* RNAi, 22.2% reduction of *CDC10* for *CDC10* RNAi, 54.3% reduction of *CDC12* for *CDC12* RNAi, and 43.4% reduction of *ASPE* for *ASPE* RNAi strains when compared to controls (Fig. 4). Although the morphologic appearance of *CDC3*, *CDC10*, and *CDC12* RNAi strains were similar, knockdown of non-targeted septins did not occur (Fig. 4).

The large size of the misshapen yeast along with a slow growth rate at 37°C (Fig. 5) suggested a defect in cytokinesis in knockdown strains when compared to controls. In yeast, nuclear and cellular divisions are often coordinated and disruption of septins in *U. maydis, C. neoformans*, and *S. cerevisiae* can result in accumulation of nuclei [14,16,32]. We used sytox green to stain and quantify *B. dermatitidis* nuclei under fluorescent microscopy. Strains knocked down for *CDC3, CDC10, CDC12,* and *ASPE* demonstrated a similar number of nuclei as reporter, non-RNAi vector control, GFPi-only controls (range 2–8 nuclei/cell). To assess for mislocalization of septa and alterations in chitin deposition, we stained control and knockdown strains with calcofluor white, which binds septal and cell wall chitin molecules. In the septin RNAi strains, cell wall chitin distribution appeared normal and misplaced septa were not present (data not shown).

RNAi of *CDC3, CDC10,* and *CDC12* alters hyphal morphology but not the phase transition

Because the interruption of septin function can impact cell morphology in a temperature-dependent manner[15,16,29], we investigated how *B. dermatitidis* septins affect morphogenesis at 22°C, as well as the phase transition. The H2AB promoter, which drives transcription of the RNAi hairpin, is active at 37°C and 22°C. Following a downshift in temperature from 37°C to 22°C, *B. dermatitidis* control and septin-RNAi strains fully converted to mold at 22°C (Fig. 2B). Knocking down *CDC3*, *CDC10*, *CDC12*, and *ASPE* did not delay the phase transition as all strains began the conversion within 24 h of 22°C incubation. Control and *ASPE* knockdown strains grew as thin, smooth, branching hyphae, whereas strains knocked down for *CDC3*, *CDC10*, and *CDC12* had curved, thick, knobby appearing hyphae (Fig. 2B). Despite abnormal hyphal appearance for *CDC3*, *CDC10*, and *CDC12* knockdown strains, chitin distribution by calcoflour staining was similar to control strains (data not shown). Previous investigation of *B. dermatitidis CDC11* demonstrated that knocking down this septin resulted in reduced production of conidia on 3M medium at 22°C. Following 14 days of incubation at 22°C on 3M medium, *CDC3*, *CDC10*, *CDC12*, and *ASPE* knockdown strains, along with control strains (reporter, non-RNAi vector control, GFPi-only), formed conidia poorly. Subsequent experiments on Bird medium improved sporulation efficiency but production of conidia was similar for septin RNAi and control strains (data not shown).

The ability for *B. dermatitidis* to convert from infectious mold to pathogenic yeast at 37°C is essential for virulence [6]. Proper septin function in *U. maydis* and *C. neoformans* contributes towards survival at elevated temperatures [15,16]. To investigate the role of *B. dermatitidis* septins on the conversion from mold to yeast, we increased the temperature from 22°C to 37°C. Knocking down *CDC3*, *CDC10*, *CDC12*, and *ASPE* did not delay the conversion to yeast when compared to controls, with all strains converting within 4 days of the upward shift in temperature. *CDC3*, *CDC10*, and *CDC12* RNAi strains still grew as misshapen yeast. *ASPE* RNAi strains grew a broad-based budding yeast, similar to control strains.

NIH-PA Author Manuscript

NIH-PA Author Manuscript

NIH-PA Author Manuscript

Discussion

Septin proteins have been identified in mammals, nematodes, insects, microsporidia, and fungi [24]. The genomes of most animals contain multiple septin-encoding genes including two in *Caenorhabditis elegans* (*UNC-59*, *UNC-61*), five in *Drosphila melanogaster* (*SEP1*, *2*, *4*, *5* and *PNUT*), and 14 for *Homo sapiens* (*SEPT1-14*) [33–35]. Similarly, fungi have multiple septin-encoding genes [24]. In *B. dermatitidis*, we have identified five septin genes including *CDC3*, *CDC10*, *CDC11*, *CDC12*, and *ASPE*. Homologs to *SHS1/SEP7*, as well as sporulation-specific septins (*SPR3*, *SPR28*) were not present in the *B. dermatitidis* genome. Comparative analysis of *B. dermatitidis*, *H. capsulatum*, *Coccidioides* spp., and *P. brasiliensis* septins revealed a high degree of conservation among the endemic dimorphic fungi. All *B. dermatitidis* septin proteins possessed GTP binding motifs (G1, G3, and G4) and a septin unique element. Three *B. dermatitidis* septins (CDC3, CDC11, CDC12) were predicted to have coiled-coil domains at the C-terminal region. The presence of a coiled-coil domain in CDC11 was unusual because the majority of CDC11 homologs (82.7%) analyzed by Pan and colleagues lacked this domain [24]. ASPE, which was first identified in *A. nidulans*, has been primarily described in filamentous fungi [13,36] and in *B. dermatitidis* lacks the N-terminal polybasic region, which is similar to ASPE homologs in other fungi.

RNA interference of *B. dermatitidis CDC3, CDC10*, and *CDC12* resulted in misshapen yeast cells with bean-like, irregular ovoid, and elongated morphologies. These abnormalities were similar to *B. dermatitidis CDC11* knockdown strains [12]. This finding was not expected because the phenotype is often specific for the mutated septin gene in most fungi [14,17,37]. Although this similarity was unanticipated, it is not unprecedented. *U. maydis SEP1-4* null mutants have nearly identical morphologic abnormalities at 28°C [15]. The overlap in phenotypes for *B. dermatitidis* strains knocked down for *CDC3*, *CDC10* and *CDC12* is unlikely to be related to inadvertent RNAi of non-targeted septin genes. Analysis of transcript abundance by qRT-PCR demonstrated only the specific septin targeted by RNAi had reduced transcription. Interestingly, a reduction in *CDC10* transcript was associated with an increase in transcription of *CDC3*, *CDC11*, *CDC12*, and *ASPE*. This may suggest a compensatory response in which ternary complexes (i.e., CDC3-CDC11-CDC12) are formed in response to altered stoichiometry of proteins in the septin filament [38].

Fungal septins are involved with the formation of the yeast bud and cytokinesis [14,37,39]. *B. dermatitidis* knocked down for *CDC3*, *CDC10*, and *CDC12* yeast were defective in budding and cytokinesis. The aberrant ovoid, bean-shaped, and elongated cells appear as though they are attempting to undergo budding, but the ‘daughter cells’ fail to undergo proper development, which is likely related to impaired cell division. The large size of *CDC3*, *CDC10*, and *CDC12* knockdown strains and slow growth rate suggest defective cytokinesis. Chitin staining did not reveal misplaced septa, which has been observed in *U. maydis* septin mutants [15].

Many pathogenic fungi are capable of yeast and filamentous growth. The impact of septins on the conversion from yeast to hyphal growth is often species specific and heterogenous. *U. maydis SEP1-4* null mutants have defective filamentation under *in vitro* inducing conditions (1% corn oil or 1% Tween 40), but are able to form filaments during plant infection [15,32]. *C. neoformans CDC3* Δ and *CDC12* Δ fail to develop hyphae on V8 medium, but have filamentous growth on MS medium [16]. For *C. albicans*, both *CDC10* Δ and *CDC11* Δ yeast convert to hyphae under inducing conditions (20% serum, 37°C) [17]. We found that *B. dermatitidis* yeast knocked down for *CDC3*, *CDC10*, *CDC12*, or *ASPE* convert to mold at environmental temperature (22°C), but the morphologies of *CDC3*, *CDC10*, and *CDC12* knockdown strains were aberrant and consisted of curved hyphae with a knobbed appearance. This aberrant pattern of curved filamentous growth has also been observed in *C.*

NIH-PA Author Manuscript

NIH-PA Author Manuscript

NIH-PA Author Manuscript

albicans and *U. maydis* null mutants [17,32,40]. The knobs may represent sites where hyphal branches started, but failed to develop.

The effect of septin gene mutations on morphology and growth can be impacted by temperature. Deletion of *U. maydis SEP1-4* results in cell lysis at 34°C, while at lower temperatures the cells are swollen with misplaced septa (28°C) or have a normal cigar shape (22°C) [15]. Similarly, septin genes in *C. neoformans* (*CDC3*, *CDC11*, *CDC12*) and *S. cerevisiae* (*CDC10*, *CDC11*) influence thermotolerance, with the deletion of these genes resulting in aberrant morphology and cell death at 37°C [16,29]. For *C. albicans*, abnormal yeast morphology was observed only at elevated temperatures for *CDC10* Δ null mutants [17]. In contrast, the morphologic abnormalities in *B. dermatitidis CDC3*, *CDC10*, and *CDC12* knockdown strains were present at both elevated and low temperatures. Moreover, the conversion from mold to pathogenic yeast at 37°C was unaffected in septin RNAi strains. Our results suggest that septin genes in *B. dermatitidis* influence morphogenesis at core human body and environmental temperatures, but are not required for the phase transition.

Although knocking down *B. dermatitidis* septins *CDC3*, *CDC10*, and *CDC12* impact morphology, there are some limitations in this study. First, RNA interference does not completely abrogate transcript abundance, which may have hindered our ability to detect subtle phenotypic differences between the knockdown strains. We selected RNA interference over gene deletion because of the low rate of homologous recombination in *B. dermatitidis* (0.04%) and the high probability that one or more septin genes would be essential [7,12,17,41]. There was a 22–78% decrease in transcript abundance in septin knockdown strains when compared to controls. Despite transcript reduction not achieving statistical significance, the morphology and growth of multiple *CDC3*, *CDC10*, and *CDC12* RNAi strains was markedly different (adjusted P value < 0.05) when compared to controls (reporter, non-RNAi vector, GFPi-only). This indicated that septin transcript abundance fell below a threshold required for normal cellular function. Moreover, when there was a loss of RNAi in a septin knockdown strain, GFP fluorescence increased and there was reversion to normal yeast morphology (data not shown). Collectively, our data supports the impact of *CDC3*, *CDC10*, *CDC12* on morphology and growth of *B. dermatitidis*. Second, virulence testing in a murine model of infection was precluded due to the slow growth rate of knockdown strains at 37°C in the yeast form. Septins in other fungi such as *C. albicans* and *C. neoformans* can impact virulence [16,32].

In conclusion, we have identified five septin genes in *B. dermatitidis* that are homologs of *CDC3*, *CDC10*, *CDC11*, *CDC12*, and *ASPE*. All septin proteins contained the expected motifs but *CDC11* was unusual because it was predicted to contain a coiled-coil domain, which is uncommon for this septin. Decrease of *CDC3, CDC10*, and *CDC12* transcript levels by RNA interference in yeast at 37°C resulted in impaired cytokinesis, cell morphology, and growth. A downshift in temperature to 22°C did not alleviate morphologic abnormalities and promoted the conversion of yeast to morphologically aberrant mold. These findings were similar to what we had previously observed in *CDC11* knockdown strains [12]. This was unanticipated because the phenotypes of septin mutants are often gene specific and can be influenced by temperature. Knocking down *ASPE* did not impact the morphology of yeast or mold. Finally, *B. dermatitidis* septins do not contribute to thermotolerance and their role in cytokinesis is not required for the conversion between yeast and mold.

Acknowledgments

Funding for this research was from the National Institutes of Health (5K08AI071004).

NIH-PA Author Manuscript

NIH-PA Author Manuscript

NIH-PA Author Manuscript

We thank Jens Eickhoff for his assistance with the statistical analysis.

References

1. Gauthier GM, Klein BS. Insights into fungal morphogenesis and immune evasion. Microbe. 2008; 3:416–423. [PubMed: 20628478]
2. Wheat LJ, Slama TG, Eitzen HE, et al. A large urban outbreak of histoplasmosis: clinical features. Ann Intern Med. 1981; 94:331–337. [PubMed: 7224378]
3. Schneider E, Hajjeh RA, Spiegel RA, et al. A coccidioidomycosis outbreak following the Northridge, Calif, earthquake. JAMA. 1997; 277:904–908. [PubMed: 9062329]
4. Klein BS, Tebbets B. Dimorphism and virulence in fungi. Curr Opin Microbiol. 2007; 10:314–319. [PubMed: 17719267]
5. Gauthier GM, Safdar N, Klein BS, Andes DR. Blastomycosis in solid organ transplant recipients. Transpl Infect Dis. 2007; 9:310–317. [PubMed: 17428278]
6. Nemecek JC, Wuthrich M, Klein BS. Global control of dimorphism and virulence in fungi. Science. 2006; 312:583–588. [PubMed: 16645097]
7. Gauthier GM, Sullivan TD, Gallardo SS, et al. SREB, a GATA transcription factor that directs disparate fates in *Blastomyces dermatitidis* including morphogenesis and siderophore biosynthesis. PLoS Pathog. 2010; 6:e1000846. [PubMed: 20368971]
8. Nguyen VQ, Sil A. Temperature-induced switch to the pathogenic yeast form of *Histoplasma capsulatum* requires Ryp1, a conserved transcriptional regulator. Proc Natl Acad Sci USA. 2008; 105:4880–4885. [PubMed: 18339808]
9. Webster RH, Sil A. Conserved factors Ryp2 and Ryp3 control cell morphology and infectious spore formation in the fungal pathogen *Histoplasma capsulatum*. Proc Natl Acad Sci USA. 2008; 105:14573–14578. [PubMed: 18791067]
10. Todd RB, Greenhalgh JR, Hynes MJ, Andrianopoulos A. TupA, the *Penicillium marneffei* Tup1 homologue, represses both yeast and spore development. Mol Microbiol. 2003; 48:85–94. [PubMed: 12657047]
11. Longtine MS, Bi E. Regulation of septin organization and function in yeast. Trends Cell Biol. 2003; 13:403–409. [PubMed: 12888292]
12. Krajaejun T, Gauthier GM, Rappleye CA, Sullivan TD, Klein BS. Development and application of a green fluorescent protein sentinel system for identification of RNA interference in *Blastomyces dermatitidis* illuminates the role of septin in morphogenesis and sporulation. Eukaryot Cell. 2007; 6:1299–1309. [PubMed: 17496124]
13. Juvvadi PR, Fortwendel JR, Rogg LE, Steinbach WJ. Differential localization of septins during growth of the human fungal pathogen *Aspergillus fumigatus* reveal novel functions. Biochem Biophys Res Commum. 2011; 415:238–243.
14. Hartwell LH. Genetic control of the cell division cycle in yeast IV. Genes controlling bud emergence and cytokinesis. Exp Cell Res. 1971; 69:245–276.
15. Alverez-Tabares I, Perez-Martin J. Septins from the phytopathogenic fungus *Ustilago maydis* are required for proper morphogenesis but dispensable for virulence. PLoS One. 2010; 5:e12933. [PubMed: 20885997]
16. Kozubowski L, Heitman J. Septins enforce morphogenetic events during sexual reproduction and contribute to virulence of *Cryptococcus neoformans*. Mol Microbiol. 2010; 75:658–675. [PubMed: 19943902]
17. Warenda AJ, Konopka JB. Septin function in *Candida albicans* morphogenesis. Mol Biol Cell. 2002; 13:2732–2746. [PubMed: 12181342]
18. McVeigh I, Morton K. Nutritional studies of *Histoplasma capsulatum*. Mycopath Mycol Appl. 1965; 25:294–308.
19. Worsham PL, Goldman WE. Quantitative plating of *Histoplasma capsulatum* without addition of conditioned medium or siderophores. J Med Vet Mycol. 1988; 26:137–143. [PubMed: 3171821]
20. Sullivan TD, Rooney PJ, Klein BS. *Agrobacterium tumefaciens* integrates transfer DNA into a single chromosomal site of dimorphic fungi and yields homokaryotic progeny from multinucleate yeast. Eukaryot Cell. 2002; 1:895–905. [PubMed: 12477790]

NIH-PA Author Manuscript

NIH-PA Author Manuscript

NIH-PA Author Manuscript

21. McDonough ES, Wisniewski TR, Penn LA, Chan DM, McNamara WI. Preliminary studies on conidial liberation of *Blastomyces dermatitidis* and *Histoplasma capsulatum*. Sabouraudia. 1976; 14:199–204. [PubMed: 959945]
22. Metzenberg RL. Bird medium: an alternative to Vogel medium. Fung Gen Newslet. 2004; 51:19–20.
23. Livak KJ, Schmittgen TD. Analysis of relative gene expression data using real-time quantitative PCR and the $2^{-\Delta\Delta Ct}$ method. Methods. 2001; 24:402–408. [PubMed: 11846609]
24. Pan F, Malmberg RL, Momany M. Analysis of septins across kingdoms reveals orthology and new motifs. BMC Evol Biol. 2007; 7:103. [PubMed: 17601340]
25. Mino M, Tanaka K, Kamei T, et al. Shs1p: a novel member of septin that interacts with Spa2p, involved with polarized growth in *Saccharomyces cerevisiae*. Biochem Biophys Res Commun. 1998; 251:732–736. [PubMed: 9790978]
26. Ozsarac N, Bhattacharyya M, Dawes IA, Clancy MJ. The *SPR3* gene encodes a sporulation-specific homologue of the yeast *CDC3/10/11/12* family of bud neck microfilaments and is regulated by ABFI. Gene. 1995; 164:157–162. [PubMed: 7590307]
27. De Virgilio C, Demarini DJ, Pringle JR. *SPR28*, a sixth member of the septin gene family in *Saccharomyces cerevisiae* that is expressed specifically in sporulating cells. Microbiology. 1996; 142:2897–2905. [PubMed: 8885406]
28. Versele M, Gullbrand B, Shulewitz MJ, et al. Protein–protein interactions governing septin heteropentamer assembly and septin filament organization in *Saccharomyces cerevisiae*. Mol Biol Cell. 2004; 15:4568–4583. [PubMed: 15282341]
29. Casamayor A, Synder M. Molecular dissection of a yeast septin: distinct domains are required for septin interaction, localization and function. Mol Cel Biol. 2003; 23:2767–2777.
30. Momany, M.; Pan, F.; Malmberg, RL. Evolution and conserved domains of the septins. In: Hall, PA.; Russell, SHE.; Pringle, JR., editors. The Septins. 1. New York: Wiley-Blackwell; 2008. p. 35-45.
31. Wolf E, Kim PS, Berger B. Multicoil: a program for predicting two- and three-stranded coiled coils. Protein Sci. 1997; 6:1179–1189. [PubMed: 9194178]
32. Boyce KJ, Chang H, D'Souza CA, Kronstad JW. An *Ustilago maydis* septin is required for filamentous growth in culture and for full symptom development on Maize. Euk Cell. 2005; 4:2044–2056.
33. Nguyen TQ, Sawa H, Okano H, White JG. The *C. elegans* septin genes, unc-59 and unc-61, are required for normal postembryonic cytokineses and morphogenesis, but have no essential function in embryogenesis. J Cell Sci. 2000; 113:3825–3837. [PubMed: 11034910]
34. Adam JC, Pringle JR, Peifer M. Evidence of functional differentiation among *Drosophila* septins in cytokinesis and cellularization. Mol Biol Cell. 2000; 11:3123–3135. [PubMed: 10982405]
35. Nakahira M, Macedo JN, Seraphim TV, et al. A draft of the human septin interactome. PLoS One. 2010; 5:e13799. [PubMed: 21082023]
36. Momany M, Zhao J, Lindsey R, Westfall PJ. Characterization of the *Aspergillus nidulans* septin (*asp*) gene family. Genetics. 2001; 157:969–977. [PubMed: 11238387]
37. An H, Morrell JL, Jennings JL, Link AJ, Gould KL. Requirements of fission yeast septins for complex formation, localization, and function. Mol Biol Cell. 2004; 15:5551–5564. [PubMed: 15385632]
38. Farkasovsky M, Herter P, Beater V. Wittinghofer. Nucleotide binding and filament assembly of recombinant yeast septin complexes. Biol Chem. 2005; 386:643–656. [PubMed: 16207085]
39. Roncero C, Sanchez Y. Cell separation and the maintenance of the cell integrity during cytokinesis in yeast: the assembly of septum. Yeast. 2010; 27:521–530. [PubMed: 20641019]
40. Warenda AJ, Kauffman S, Sherrill TP, Becker JM, Konopka JB. *Candida albicans* septin mutants are defective for invasive growth and virulence. Infect Immun. 2003; 71:4045–4051. [PubMed: 12819094]
41. Momany M, Hamer JE. The *Aspergillus nidulans* septin encoding gene, *aspB*, is essential for growth. Fungal Genetic Biol. 1997; 21:92–100.

NIH-PA Author Manuscript

NIH-PA Author Manuscript

NIH-PA Author Manuscript

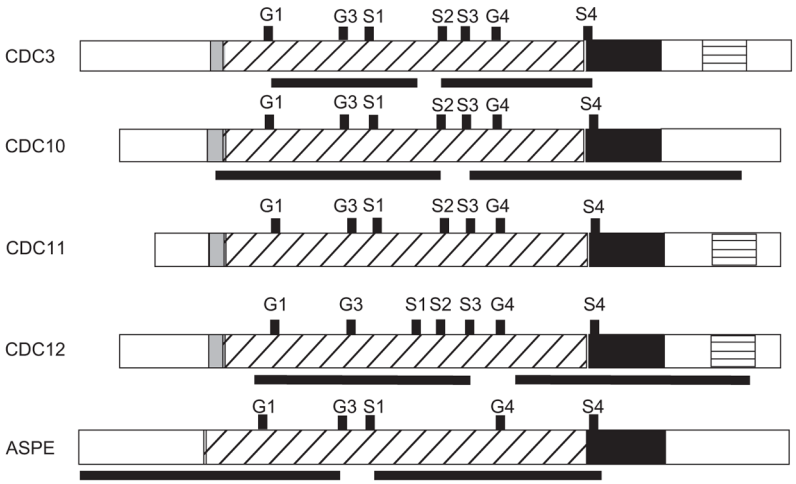

Fig. 1.

Septin regions targeted for RNA interference. Black bars below *CDC3, CDC10, CDC12*, and *ASPE* correspond to the regions targeted for RNA interference. In addition, conserved motifs (G1, G3, G4, S1-S4), GTPase domain, polybasic region, septin unique element, and coiled-coil domains are shown for all septins. The polybasic region is shaded gray. Diagonal lines represent the GTPase domain. The septin unique element is black. Horizontal lines indicate the coiled-coil domain.

NIH-PA Author Manuscript
NIH-PA Author Manuscript
NIH-PA Author Manuscript

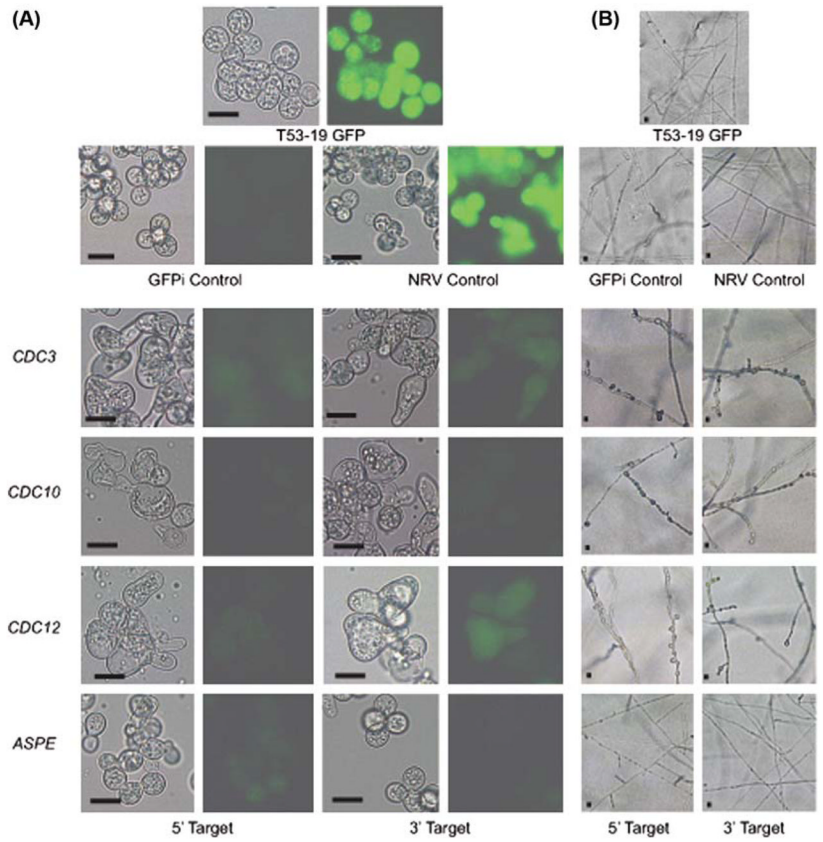

Fig. 2.

Phenotype of *CDC3*, *CDC10*, *CDC12*, & *ASPE* knockdown strains at 37°C and 22°C. (A) T53-19 GFP (reporter) and non-RNAi vector (NRV) control strains grew as broad-based budding yeast with intense green fluorescence. GFP RNAi only (GFPi) control displayed normal yeast morphology, but reduced GFP intensity. *CDC3*, *CDC10*, and *CDC12* knockdown strains grew as large, misshapen yeast with reduced GFP intensity. ASPE-GFP knockdown strains had reduced GPF intensity and similar morphology to the control strains. Scale bar is 10 μm. Cells were grown on 3M agar at 37°C. (B) Following a downshift in temperature from 37°C to 22°C, control strains grew as thin, smooth, branched hyphae. In contrast, *CDC3*, *CDC10* and *CDC12* knockdown strains grew as curved mold with a knobby appearance. *ASPE* RNAi strains have a similar morphology as the control strains. Corresponding fluorescent images are not shown for hyphal cells because GFP, which functions as a reporter, is under control of the BAD-1 promoter and is not expressed at 22°C. The H2AB promoter, which drives transcription of the hairpin responsible for RNA interference is active at both 37°C and 22°C. Scale bar is 10 μm. Cells were grown on 3M agar at 22°C.

NIH-PA Author Manuscript

NIH-PA Author Manuscript

NIH-PA Author Manuscript

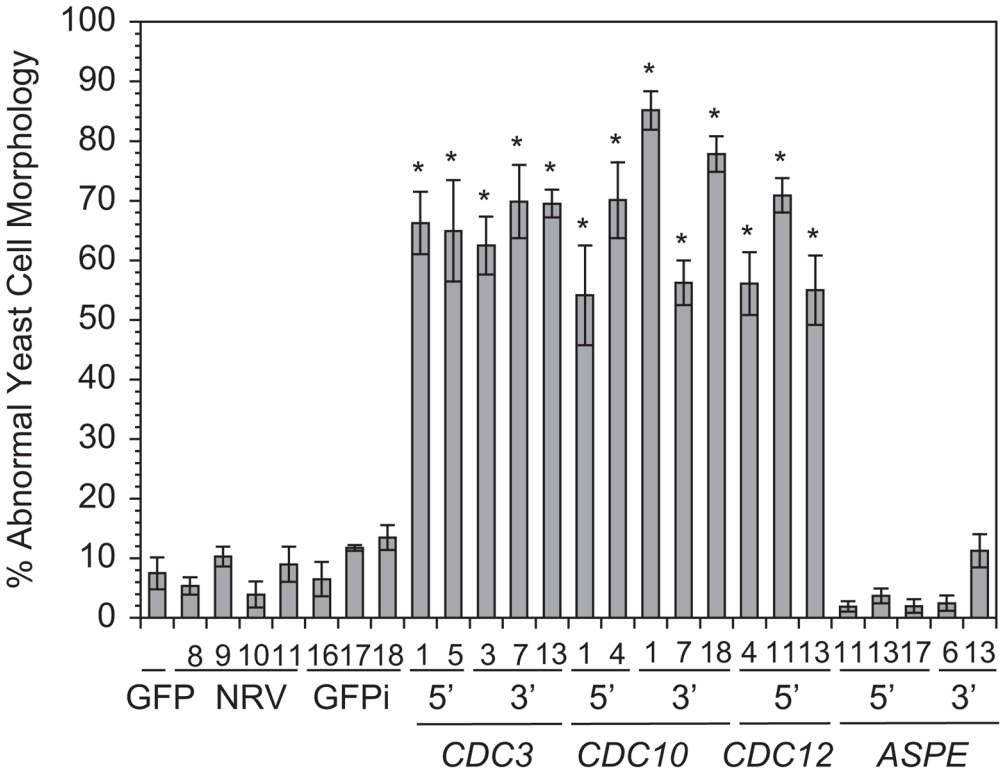

Fig. 3.

Quantification of abnormal yeast morphology in septin knockdown strains. The majority of yeast cells for *B. dermatitidis* strains knocked down for *CDC3*, *CDC10*, and *CDC12* had abnormal morphology (55–85%) when compared to control strains (<15%). This difference was statistically significant (adjusted *P* value <0.05; represented by an asterisk). *ASPE* knockdown strains grew as normal shaped yeast similar to controls. At least 400 cells were analyzed per strain. Numbers below the histogram bars represent the different transformants that were analyzed. 5′ and 3′ refer to the gene region targeted for RNA interference. GFP is the GFP reporter strain (T53-19 GFP). GFPi refers to the control strain knocked down for GFP only and NRV refers to the non-RNAi vector control.

NIH-PA Author Manuscript

NIH-PA Author Manuscript

NIH-PA Author Manuscript

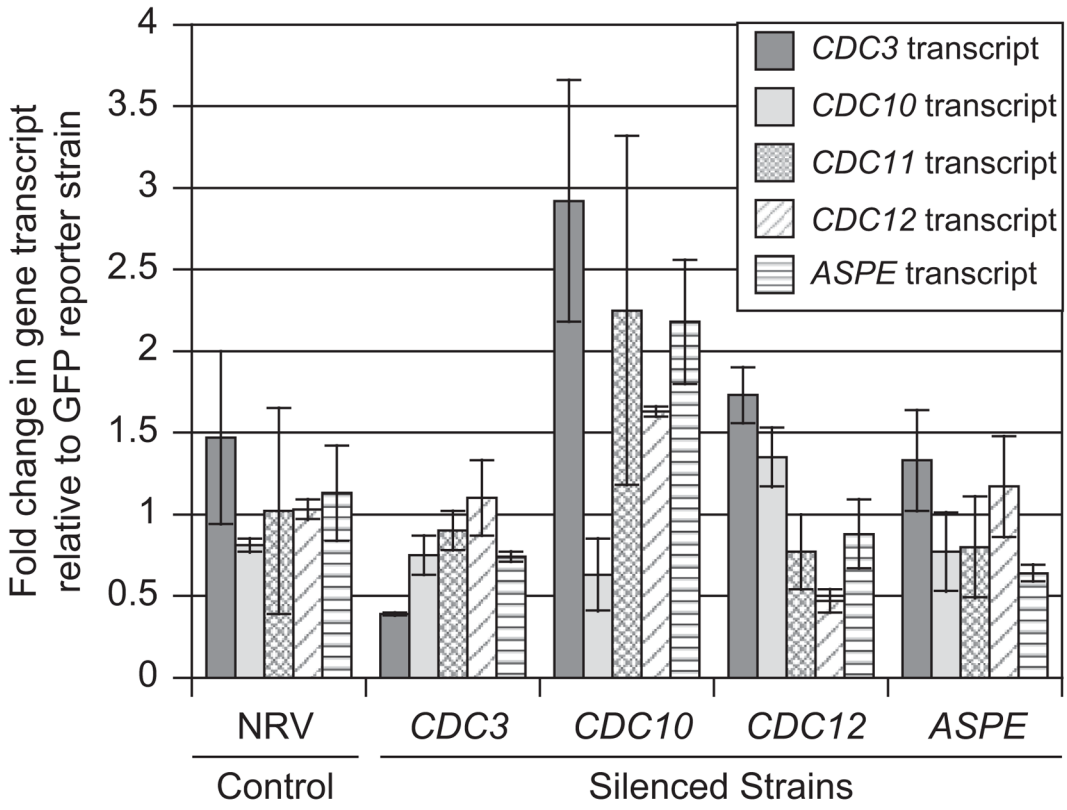

Fig. 4.

Quantitative real-time PCR analysis. qRT-PCR demonstrated a reduction in transcript abundance for *CDC3*, *CDC10*, *CDC12*, and *ASPE* for their respective knockdown strains when compared to GFP reporter and non-RNAi vector (NRV) control strains. NRV control had similar transcript levels to the reporter strain. Quantitative RT-PCR data was analyzed using the $2^{-\Delta\Delta Ct}$ method and values are expressed as fold change in gene transcript relative to the GFP reporter strain. Ct values were normalized to α-tubulin with ΔCt = (Ct of gene of interest) − (Ct of α-tubulin). ΔΔCt = (ΔCt of NRV or knockdown strain) − (ΔCt of GFP reporter). ANOVA was used to analyze transcript abundance between septin knockdown strains and controls. Transcript reduction in knockdown strains was not statistically significant when compared to controls; however, the sharp differences in morphology between knockdown and controls indicated that septin transcript in knockdown strains fell below a threshold required for normal cellular function.

NIH-PA Author Manuscript

NIH-PA Author Manuscript

NIH-PA Author Manuscript

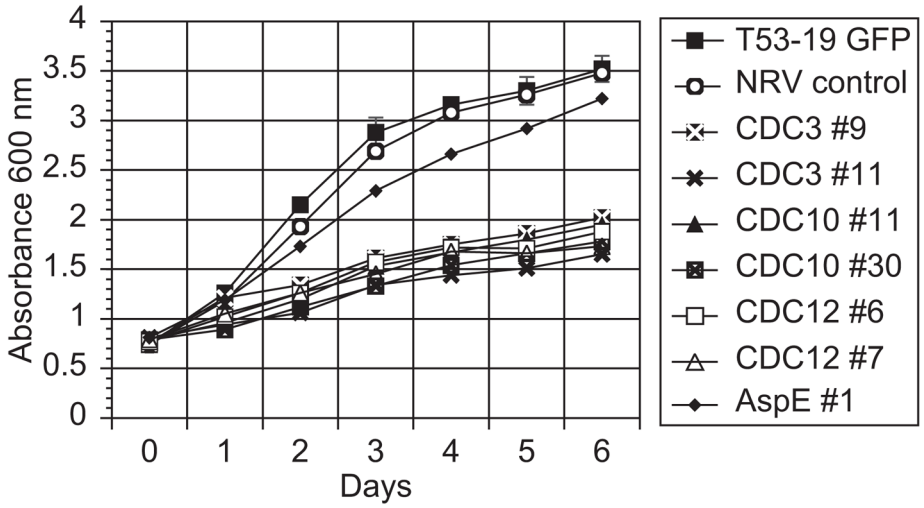

Fig. 5.

Growth curve for septin knockdown strains. At 37°C, yeast strains knocked down for *CDC3*, *CDC10*, and *CDC12* grew substantially slower than T53-19 GFP reporter and non-RNAi vector control strains. *ASPE* knockdown yeast grew faster than other septin RNAi strains, but slower than control strains. By day 2 in liquid culture, all septin knockdown strains demonstrated a statistically significant reduction in growth when compared to the reporter and non-RNAi controls (adjusted *P* value < 0.05). Yeast cultures were grown in liquid HMM medium over a period of 6 days and growth was measured daily by absorbance at 600 nm. Numbers next to *CDC3, CDC10, CDC12*, and *ASPE* represent the strains analyzed. A representative experiment is shown.

NIH-PA Author Manuscript NIH-PA Author Manuscript NIH-PA Author Manuscript

Table 1

Comparison of *Blastomyces dermatitidis* septins against other dimorphic fungi.

	H. capsulatum			***P. brasiliensis***		
***B. dermatitidis* Septin**	**HS**	**Identity**	**Similarity**	**HS**	**Identity**	**Similarity**
CDC3	896	98.0%	99.0%	903	93.7%	95.7%
CDC10	671	97.0%	98.0%	664	95.0%	97.0%
CDC11	681	99.7%	100.0%	663	97.0%	99.0%
CDC12	747	96.7%	97.6%	748	97.0%	97.0%
ASPE	795	87.3%	92.0%	865	76.7%	84.0%
	C. immitis			*C. posadasii*		
B. dermatitidis Septin	HS	Identity	Similarity	HS	Identity	Similarity
CDC3	760	92.0%	95.0%	848	92.0%	95.0%
CDC10	633	92.2%	94.0%	646	94.0%	95.0%
CDC11	612	91.8%	95.5%	623	91.0%	95.0%
CDC12	594	88.5%	92.0%	721	94.0%	96.0%
ASPE	539	66.5%	74.0%	654	61.0%	70.0%

B. dermatitidis septin amino acid sequences were compared to *H. capsulatum* (strains G186R, H88, Nam1), *P. brasiliensis* (strains Pb01, Pb03, Pb18), *C. immitis* (strains H538, RS, RMSCC 3703, RMSCC 2394), and *C. posadasii* (strains Silveira, RMSCC 3488) using protein-protein blast from the Broad Institute (www.broadinstitute.org). HS refers to high score.

Med Mycol. Author manuscript; available in PMC 2013 March 25.